Journal of Marine Research, 63, 159–185, 2005

The material derivative of neutral density

by Trevor J. McDougall[1,2] and David R. Jackett[1]

ABSTRACT

An expression for the rate of change of neutral density following a fluid parcel (the material derivative) is derived and checked numerically. This expression can be used to quantify the degree to which neutral density varies even under purely adiabatic and isohaline motions. We also present an approximate form of neutral density, namely a rational function of only two variables, either salinity and conservative temperature or salinity and potential temperature.

1. Introduction

Turbulent motions in the ocean interior are highly constrained by the vertically stratified nature of the ocean's density field, and the energetic mesoscale eddies are not thought to cause significant diapycnal mixing. Rather, mass and other properties are stirred and mixed efficiently along isopycnals by the mesoscale eddies, leaving much weaker processes to accomplish the diapycnal diffusion and diapycnal advection in the ocean interior.

Because the lateral diffusivity of mixing processes acting along isopycnals is approximately eight orders of magnitude larger than the diapycnal diffusivity that operates in the ocean interior, it is important to have an accurate procedure for evaluating the appropriate "isopycnal" surface in which the strong lateral mixing occurs. It is straightforward to define a local neutral tangent plane in which parcels can be moved small distances without experiencing vertical buoyant restoring forces. But defining horizontally extensive surfaces that are "neutral" is far from a trivial exercise, and the options for approximately neutral surfaces range from potential density surfaces, patched potential density surfaces (Reid and Lynn, 1971), neutral density surfaces (Jackett and McDougall, 1997) and orthobaric density surfaces (de Szoeke *et al.,* 2000).

These surfaces differ in the extent to which they achieve the three desirable but mutually inconsistent objectives of (i) being as neutral as possible, (ii) being as quasi-material as possible, and (iii) possessing a geostrophic streamfunction (commonly called a Montgomery potential). The quasi-material concept needs explanation: a density variable is said to be quasi-material if it is a function of only salinity and potential temperature. In this case, when vertical heaving motion causes water parcels to undergo a change of pressure there is no flow through the density surface. Such dia-surface flow is only due to irreversible

1. CSIRO Marine Research, Castray Esplande, Hobart, Tasmania 7000, Australia.
2. Corresponding author. ***email: trevor.mcdougall@csiro.au***

mixing processes if the density variable is quasi-material. If a surface is not quasi-material, then even an adiabatic and isohaline change in pressure will result in the flow of seawater through the surface.

The relative importance that oceanographers place on these three properties (neutrality, quasi-materiality and the existence of a geostrophic streamfunction) depends on the application. For example, the layered modeling community has to date required the exact observance of quasi-materiality, thus necessarily suffering a penalty on the score of neutrality and also not possessing an exact geostrophic streamfunction. The approach taken by Jackett and McDougall (1997) in forming the algorithm for the neutral density variable was to make neutral density surfaces as neutral as possible while making no attempt at achieving a geostrophic streamfunction. The extent of the quasi-material nature of neutral density has not been addressed in the literature to date, and spurred on by interest in this question from Dr Roland de Szoeke, we address this issue in the present manuscript.

We begin in Section 2 with a discussion of the observational evidence that the strong lateral mixing occurs along neutral tangent planes. The next section examines the patched potential density procedure of Reid and Lynn (1971) for forming approximately neutral surfaces. We show that as the patching is done at ever finer intervals of space, the patched potential density surface attains the neutral property. In Sections 4–7 we establish the expressions for the material derivative of neutral density, and then in Sections 8–9 we form a new approximate form of neutral density which is a function only of salinity and one of either conservative temperature or potential temperature.

2. Evidence for epineutral mixing

The smallness of the dissipation of mechanical energy in the ocean interior provides the strongest evidence that the lateral mixing of mesoscale eddies occurs along the neutral tangent plane. If the lateral diffusivity $\kappa \approx 10^3\,\mathrm{m^2\,s^{-1}}$ of mesoscale dispersion and subsequent molecular diffusion were to occur along a surface that differed in slope from the neutral tangent plane by an angle whose tangent was s, then the individual fluid parcels would be transported above and below the neutral tangent plane and would need to sink or rise in order to attain a vertical position of neutral buoyancy. This vertical motion would either (i) involve no small-scale turbulent mixing, in which case the combined process is equivalent to epineutral mixing, or (ii), the sinking and rising parcels would mix and entrain in a plume-like fashion with the ocean environment, so suffering irreversible diffusion. If this second case were to happen, the dissipation of mechanical energy associated with the diapycnal mixing would be observed. But in fact the dissipation of mechanical energy in the main thermocline is consistent with a diapycnal diffusivity of only $10^{-5}\,\mathrm{m^2\,s^{-1}}$ (Toole and McDougall, 2001). This small value of the diapycnal diffusivity has been confirmed by purposely released tracer experiments.

Even if all of this observed diapycnal diffusivity were due to mesoscale eddies mixing along a direction different to neutral tangent planes, the (tangent of the) angle between this mesoscale mixing direction and the neutral tangent plane, s, would satisfy $10^{-5}\,\mathrm{m^2\,s^{-1}} = s^2\kappa$ and using $\kappa \approx 10^3\,\mathrm{m^2\,s^{-1}}$ gives the maximum value of the angle s to be 10^{-4}. Since

we believe that bona fide interior diapycnal mixing processes (such as breaking internal gravity waves) are responsible for the bulk of the observed diapycnal diffusivity, we conclude that the angular difference between the direction of mesoscale eddy mixing and the neutral tangent plane must be substantially less than 10^{-4}; say 2×10^{-5} for argument's sake. This means that as ocean modelers we need to have the strong lateral mixing occurring along directions that differ from neutral tangent planes by no more than this angle, and this is a rather stringent requirement unless a deliberately rotated diffusion tensor is used (Griffies *et al.,* 1998).

3. The approach to neutrality of patched potential density surfaces

The method of Reid and Lynn (1971) of forming "isopycnal" surfaces involves using potential density surfaces referenced to a series of pressures, usually 0 db, 1000 db, 2000 db, 3000 db and 4000 db. At the mid-point pressures 500 db, 1500 db, 2500 db and 3500 db, the potential densities referenced to the neighboring reference pressures are matched so that the average water mass at the mid-point pressure lies on both the potential density surfaces referenced to the neighboring reference pressures. Here we investigate how closely this definition of a patched potential density "isopycnal" approaches a neutral trajectory. We restrict attention to the case where there is no helicity of the neutral direction and hence no path-dependence in the definition of a neutral surface. Helicity is defined as $\mathbf{n} \cdot \nabla \times \mathbf{n}$ where $\mathbf{n} = \alpha \nabla \Theta - \beta \nabla S$ is everywhere normal to the neutral tangent planes, and McDougall and Jackett (1988) have shown that helicity is proportional to $\nabla p \cdot \nabla S \times \nabla \Theta$. If one takes a meridional section (say from the Atlantic) and assumes that this section is characteristic of the whole ocean basin, that is that the ocean is independent of longitude, then one effectively is assuming that the helicity is zero since all of ∇p, ∇S and $\nabla \Theta$ lie in the $y - z$ plane so the triple product $\nabla p \cdot \nabla S \times \nabla \Theta$ is zero.

An oceanic cross-section in the upper 1000 db is sketched in Figure 1. The potential density surface, σ_0, referenced to the sea surface is shown, being tangential to the neutral trajectory at $p = 0$ db, while a potential density surface σ_1 (referenced to 1000 db) is shown tangent to the neutral trajectory at 1000 db. These two potential density surfaces are shown meeting at a pressure other than 500 db at point F. If these two potential density surfaces met at 500 db then it seems clear that the patched potential density or "isopycnal" surface of Reid and Lynn (1971) and of Reid (1994) would probably be as good an approximation to a neutral trajectory as could be achieved with the given increment of 1000 db between successive reference pressures. But the matching procedure of Reid (1994) does not guarantee that the osculating potential density surfaces from points A and B meet at 500 db. In general these osculating potential density surfaces meet at another pressure, such as at point F in Figure 1(a). Proceeding from the surface outcrop point A, the matching procedure of Reid (1994) has the initial σ_0 surface connecting to the dashed σ_1 surface at point D in Figure 1(a). Here we quantify the systematic offset between the patched potential density surfaces of Reid (1994) and the neutral trajectory by quantifying the offset between the dashed σ_1 surface and the σ_1 surface through point B at 1000 db. That is, we quantify the density difference that underlies why points D and E do not coincide.

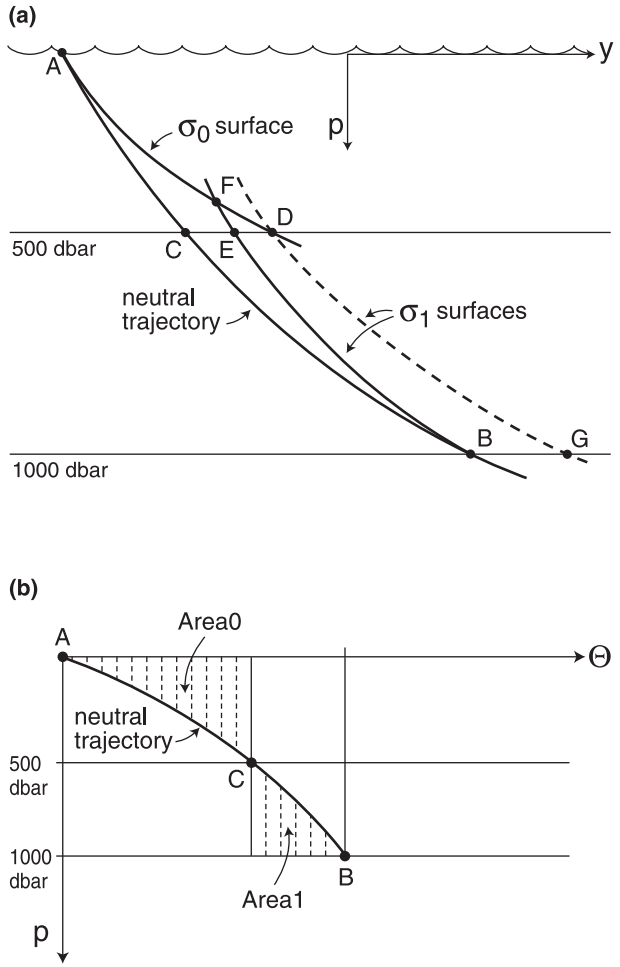

Figure 1. (a) Meridional cross-section of a neutral trajectory and some potential density surfaces that are used to quantify the extent of the neutrality of the Reid and Lynn (1971) patched potential density surface concept. (b) The areas Area0 and Area1 on the $\Theta - p$ diagram are proportional to the potential density differences $\sigma_0^C - \sigma_0^A$ and $\sigma_1^C - \sigma_1^B$ of the points A, B and C of panel (a).

The variation of potential density (referenced to the sea surface) between points A and C along the neutral trajectory of Figure 1(a) is (from (A4) of the Appendix)

$$\sigma_0^C - \sigma_0^A = \sigma_0^C - \sigma_0^D \approx 10^3 T_b \int_A^C p d\Theta = 10^3 T_b \,\text{Area0} \tag{1}$$

where Area0 is shown on Figure 1(b). Here T_b is the thermobaric parameter, $T_b = \beta\partial(\alpha/\beta)/\partial p \approx 2.7 \times 10^{-12}\ \text{K}^{-1}\ \text{Pa}^{-1}$, and it is usually sufficiently accurate to take the

thermobaric parameter to be a constant. Similarly, the difference in σ_1 between points B and C along the neutral trajectory is proportional to Area1 of Figure 1(b) since

$$\sigma_1^C - \sigma_1^B = \sigma_1^C - \sigma_1^E \approx 10^3 T_b \int_B^C (p - 1000) d\Theta = 10^3 T_b \text{ Area1}. \tag{2}$$

It is convenient to define the ratio of the horizontal gradients of conservative temperature and salinity (in terms of buoyancy) at the matching pressure as R_H where

$$R_H = \frac{\alpha}{\beta}(500)[\Theta^C - \Theta^D]/[S^C - S^D]. \tag{3}$$

Using the differential relationship $d \ln \rho_0 = \beta(0) dS - \alpha(0) d\Theta$, the temperature difference $\Theta^C - \Theta^D$ can be expressed in terms of Area0 by (using (1) and (3))

$$[\Theta^C - \Theta^D] \approx -T_b \frac{\text{Area0}}{\beta(0)} \left[\frac{\alpha}{\beta}(0) - \frac{\alpha}{\beta}(500)\frac{1}{R_H}\right]^{-1}. \tag{4}$$

The difference in σ_1 between parcels C and D can similarly be expressed as

$$\sigma_1^C - \sigma_1^D \approx -10^3[\Theta^C - \Theta^D]\beta(1000)\left[\frac{\alpha}{\beta}(1000) - \frac{\alpha}{\beta}(500)\frac{1}{R_H}\right]. \tag{5}$$

The offset in σ_1 between the patched potential density surface and the neutral trajectory is given by $\sigma_1^E - \sigma_1^D$ which can be found from (2), (4) and (5) to be

$$\sigma_1^E - \sigma_1^D \approx 10^3 T_b \text{ Area0} \frac{\beta(1000)}{\beta(0)} \left[\frac{R_H \frac{\alpha}{\beta}(1000) - \frac{\alpha}{\beta}(500)}{R_H \frac{\alpha}{\beta}(0) - \frac{\alpha}{\beta}(500)}\right] - 10^3 T_b \text{ Area1}. \tag{6}$$

The ratio α/β can be expanded about 500 db using the definition of the thermobaric parameter $T_b = \beta(\alpha/\beta)_p$ so that the offset (6) in σ_1 can be expressed as a fraction of the variation of σ_1 that occurs between 500 db and 1000 db along the neutral trajectory as

$$\frac{\sigma_1^E - \sigma_1^D}{\sigma_1^C - \sigma_1^E} \approx \frac{\text{Area0}}{\text{Area1}} \frac{\beta(1000)}{\beta(0)} \left[\frac{R_H(1 + 500 T_b/\alpha(500)) - 1}{R_H(1 - 500 T_b/\alpha(500)) - 1}\right] - 1. \tag{7}$$

Ignoring the small variation of the saline contraction coefficient with pressure, that is, taking $\beta(1000) \approx \beta(0)$, we have that

$$\frac{\sigma_1^E - \sigma_1^D}{\sigma_1^C - \sigma_1^E} \approx \frac{\text{Area0}}{\text{Area1}} \left[\frac{(1 - R_H^{-1}) + 500 T_b/\alpha(500)}{(1 - R_H^{-1}) - 500 T_b/\alpha(500)}\right] - 1 \tag{8}$$

and we note that points D and E would be coincident if the patched potential density surface was the best possible approximation to a neutral trajectory on Figure 1.

It can be shown that the large square bracket in (8) is approximately the ratio of the

horizontal gradients at 500 db of the potential densities referenced to 1000 db and 0 db, that is,

$$\left.\frac{\partial\sigma_1}{\partial\sigma_0}\right|_{p=500\text{ db}} \approx \left[\frac{(1 - R_H^{-1}) + 500T_b/\alpha(500)}{(1 - R_H^{-1}) - 500T_b/\alpha(500)}\right]. \tag{9}$$

Hence we can understand that (8) will be zero and the patched potential density surface will be as neutral as possible when the ratio of the increase in σ_0 in going from 0 db to 500 db (Area0) to the decrease in σ_1 in going from 500 db to 1000 db (Area1) is equal to the ratio of the horizontal gradients of these potential densities at 500 db.

Typically $500T_b/\alpha(500)$ is about 0.1 so that the large square bracket in (8) and (9) becomes approximately $(1.1 - R_H^{-1})/(0.9 - R_H^{-1})$ and with $R_H \approx 2$, this large square bracket is about 1.5. Hence if the areas Area0 and Area1 on Figure 1(b) were approximately equal, the offset in σ_1 (namely $\sigma_1^E - \sigma_1^D$) involved with using patched potential density would be 50% of the variation of σ_1 along the neutral trajectory between 500 db and 1000 db, namely $\sigma_1^C - \sigma_1^E$. Equivalently (8) would only be zero in these circumstances if the area ratio Area1/Area0 is 1.5.

In practice, in the Southern Ocean one finds that Area1 is smaller than Area0 so that (8) takes a value larger than 0.5 in the Reid and Lynn (1971) patched potential density procedure, meaning that this patching procedure is not the ideal patching procedure in the Southern Ocean. However, this needs to be understood in the context of alternative isopycnal definitions. For example, if the one definition of potential density were used over the complete pressure range from 0 db to 1000 db then the variation of potential density along the neutral trajectory from A to B would be the approximately triangular area under the line from A to B in Figure 1(b) which is approximately four times Area0 or Area1. Hence the density mismatch error given by (8) is approximately one eighth the error involved with using a single potential density over this 1000 db pressure range. The benefits of using Reid's patched potential density surfaces which are never more than 500 dbar distant from the reference pressure clearly increase as one considers denser surfaces that plunge to great depths in the ocean, compared with using a single definition of potential density.

In Figure 2 we show pressure, σ_Θ and γ^n on the fifth surface of Reid (1994) (see Table 1) which lies at a pressure of about 2100 dbar at low latitudes. Potential density (referred to zero pressure) increases from the southern outcrop toward the north and is a maximum under the influence of the Mediterranean Water. The extent of the neutrality of this patched potential density surface can be gauged from the contours of neutral density in Figure 2(c). As noted in the previous paragraph, the matching procedure at the 500 dbar level in the southern hemisphere leaves something to be desired. This shows up in Figure 2(c) as a significant gradient of neutral density on this "isopycnal" in the southern half of the southern hemisphere: the difference of 0.04 kg m^{-3} between neutral density values of 28.02 kg m^{-3} and 28.06 kg m^{-3} in this latitude range is not a trivial density difference.

Now we consider what would happen if the same matching procedure of Reid and Lynn (1971) were used but the pressure intervals that are used to define patched potential density

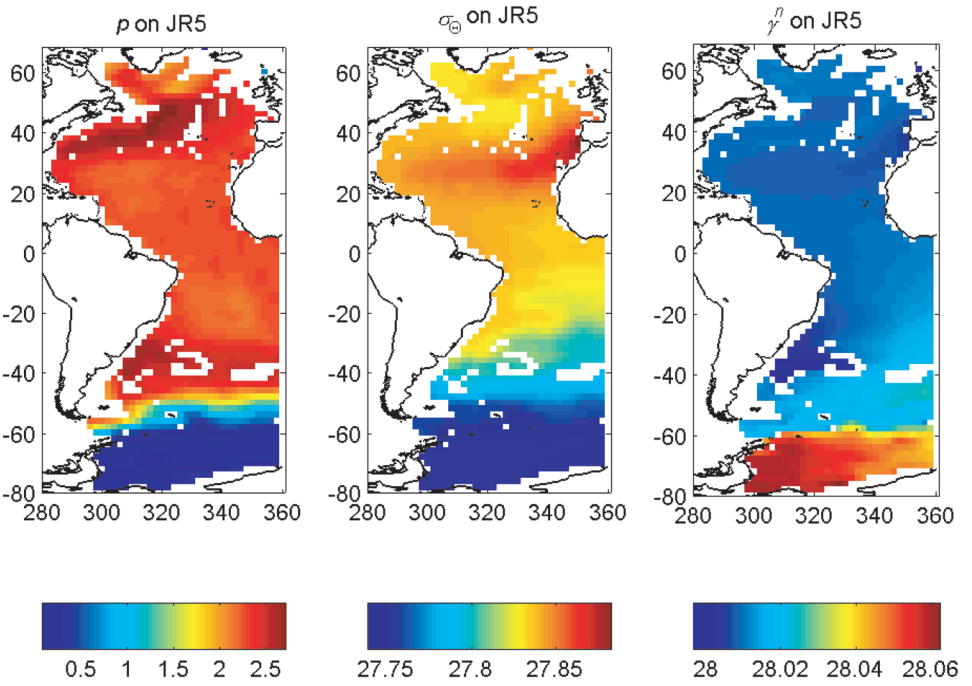

Figure 2. Pressure (a), potential density (b) and neutral density (c), plotted on the fifth "isopycnal" surface of Reid (1994).

surfaces is reduced from 1000 db toward zero. The first thing to notice is that the variation of potential density along a neutral trajectory increases as the square of the pressure interval. This can be seen from Figure 1(b) where both the pressure range and the temperature range of the approximately triangular areas Area0 and Area1 would halve if the pressure interval were halved from 1000 db to 500 db. In addition, the large square bracket in (8) and (9) would be only half as far from unity. Hence we conclude (from (8) and (2)) that as the pressure interval that is used to define the matching procedure approaches zero, the error $\sigma_1^E - \sigma_1^D$ approaches zero as the third power of the matching pressure interval. There are of course many more such matching locations; the number of which is proportional to the reciprocal of the matching pressure interval. Hence we conclude that the matching error overall goes as the square of the matching pressure interval. This serves to confirm the assertion of McDougall (1987a) that in the limit of ever finer pressure intervals of the Reid and Lynn (1971) procedure, the patched potential density surfaces so obtained approach neutral trajectories:—they do so quadratically fast.

In this section we have concentrated on the case of an ocean with zero helicity. In this case the limit of very finely-patched potential density surfaces approaches the well-defined neutral surface. The presence of a small amount of helicity in the ocean means that such well-defined neutral surfaces do not exist and so there will always be a certain amount of "discordance" between the individual leaves of patched potential density surfaces. Such a

discordance is illustrated in Figure 14 of de Szoeke *et al.* (2000). It is important to realize that this discordance is a consequence of the nonzero local value of helicity at the matching pressure of the potential densities. The different water masses that exist in the North and South Atlantic can be accommodated by the finely patched potential density concept described above (and also by neutral density) because such water mass differences between the hemispheres do not contribute to the ocean's helicity because these water mass contrasts are never adjacent to each other. Thus while salinity is not a single-valued function of pressure and *in situ* density, the different northern and southern branches of $S(p, \rho)$ are not indicative of helicity and do not cause discordances for the finely patched potential density procedure (simply because the two different branches are always well separated in space).

4. The material derivative of neutral density due to changes in pressure

The neutral density computer algorithm (Jackett and McDougall, 1997) takes an oceanic datum of salinity, temperature, pressure, latitude and longitude and labels it with a value of neutral density. This is achieved by neutrally associating the datum with certain depths on the four vertical casts of the pre-labeled atlas that are located at latitudes and longitudes which are immediately adjacent to the datum. The respective pairs of fluid parcels are deemed to be "neutrally associated" if they have the same value of potential density referenced to the average pressures of the original datum and each of the fluid parcels on the pre-labeled casts in turn. The label for the original datum is then taken as the weighted average of the neutral density labels found on the adjacent labeled casts.

Neutral density was designed so that neutral density surfaces are as neutral as possible:—the difference between the slope of the local neutral tangent plane and the neutral density surface is minimized using a relaxation technique. Another highly desired property of density surfaces is the quasi-material property (if a density variable is 100% quasi-material, then flow occurs through the "isopycnals" only in response to irreversible mixing processes (such as turbulent diapycnal mixing, double-diffusive convection, cabbeling, thermobaricity etc.)). In order to assess the degree to which neutral density is quasi-material, an expression is needed for the material derivative of neutral density, and this task is addressed in this and the following three sections.

Since neutral density (Jackett and McDougall, 1997) is a function of five variables, namely $\gamma^n = \gamma^n(S, \Theta, p, x, y)$, the material derivative of neutral density, $d\gamma^n/dt$, can be regarded as the sum of five terms, being the relevant partial derivative multiplying the five material derivatives $\dot{S}$, $\dot{\Theta}$, $\dot{p}$, u and v. The nomenclature here is mostly standard with S being the salinity on the Practical Salinity Scale, p the absolute pressure less 10.1325 dbar (Feistel, 2003), x and y being the distance in the eastward and northward directions. The temperature variable is the conservative temperature Θ of McDougall (2003) which is simply potential enthalpy divided by a constant. Conservative temperature is a function of salinity and potential temperature, $\Theta(S, \theta)$, and Θ better represents "heat" in the ocean than does potential temperature by more than two orders of magnitude.

Here the full expression for $d\gamma^n/dt$ will be constructed by first considering the influence

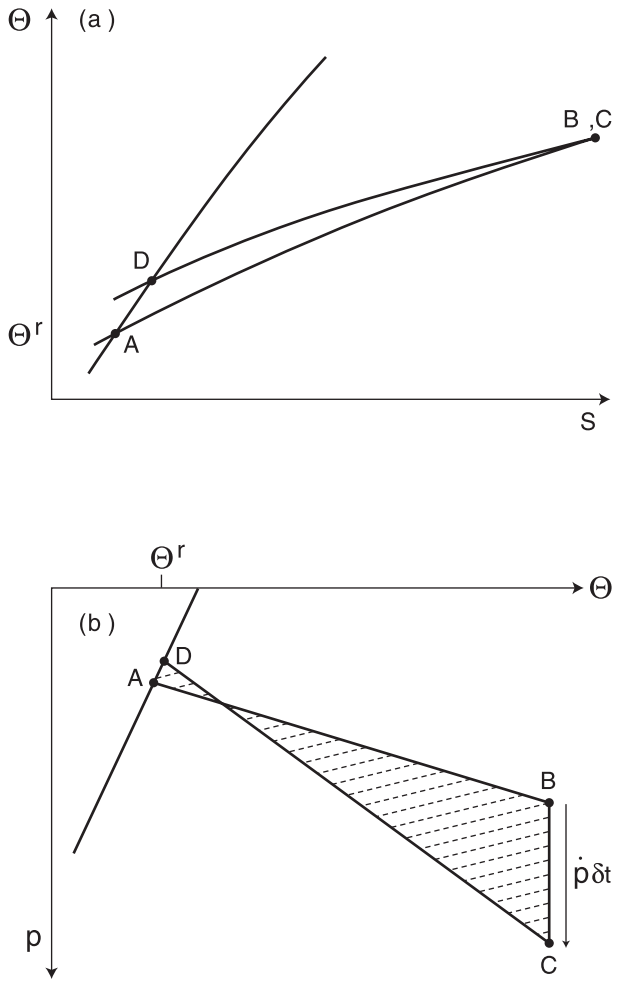

Figure 3. Salinity-conservative temperature plot (a) and temperature-pressure plot (b) of points A, B, C and D along a neutral trajectory that are used to deduce the contribution of pressure changes to the material derivative of neutral density.

of $\dot{p}$ at constant S, Θ, x and y, second, calculating the effect of the lateral movement $\mathbf{V} = (u, v) = (\dot{x}, \dot{y})$ of a fluid parcel while its S, Θ and p remain constant, then thirdly and finally (in Section 6) accounting for the effects of $\dot{S}$ and $\dot{\Theta}$ at constant p, x and y.

In order to quantify the influence of the material derivative of pressure, $\dot{p}$, on the material derivative of neutral density, refer to Figure 3(a) which depicts a fluid parcel (S^B, Θ^B, p^B) at point B communicating neutrally to the parcel A, (S^A, Θ^A, p^A) on the labeled reference cast of the neutral density algorithm. The particular reference cast is the one at the same longitude and latitude as Parcel B. Now the pressure of parcel B is increased to $p + \dot{p}\delta t$ where the parcel is now called parcel C and it communicates neutrally with parcel

D on the reference cast. Parcels C and D have the same potential density referenced to the pressure $0.5(p^D + p^B + \dot{p}\delta t)$. Consider the neutral trajectory that begins at point A and proceeds to point B, then to C then to D. These points are shown in Figure 3(b) on the $\Theta - p$ diagram.

In the Appendix we develop the expression (A4) for the lateral gradient of potential density in the neutral tangent plane, and integrating (A4) around the neutral trajectory of Figure 3(b) from point A to D we find that the difference in potential density between these two parcels is given by

$$(\rho^D_\Theta - \rho^A_\Theta)/\rho_\Theta \approx \int_A^D T_b[p - p_r]d\Theta. \tag{10a}$$

Consider now the particular potential density that is referenced to the average pressure of parcels A and D, that is, to the pressure $(p^A + p^D)/2$. Taking the thermobaric coefficient to be constant, the integral on the right of (10a) is then exactly T_b times the shaded closed area in Figure 3(b), that is, the area A-B-C-D-A enclosed on this $\Theta - p$ diagram, being the neutral trajectory A-B-C-D and the straight line joining points D and A. To lowest order in $\dot{p}\delta t$, $(p - p_r)$ and $(\Theta - \Theta^r)$ this area is the signed area of the triangle A-B-C namely $-\frac{1}{2}T_b(\Theta - \Theta^r)\dot{p}\delta t$ where $\Theta^r = \Theta^A$ is a more convenient symbol for conservative temperature on the reference cast that is neutrally connected to the parcel in question. Since $p^A - p^D$ is much less than the imposed pressure difference $\dot{p}\delta t$, this area of triangle A-B-C is a good approximation to the shaded area A-B-C-D-A. More accurately, the shaded area of Figure 3(b) is the difference between the areas of the triangles A-B-C and A-D-C, and the area of this second triangle is $\frac{1}{2}(p^A - p^D)\{(\Theta - \Theta^r) - (p - p^r)\Theta^r_p\}$ where Θ^r_p is the vertical temperature gradient on the reference cast with respect to pressure.

The ratio of the vertical gradient of neutral density to that of locally-referenced potential density defines the factor b of Jackett and McDougall (1997) (this factor varies between 0.5 and 2) so that the left-hand side of (10a) is b^{-1} times the difference between the values of $\ln \gamma^n$ for parcels D and A so that

$$[\ln \gamma^n]^D_A \approx -\frac{1}{2}bT_b(\Theta - \Theta^r)\dot{p}\delta t + \frac{1}{2}bT_b(p^A - p^D)\{(\Theta - \Theta^r) - (p - p^r)\Theta^r_p\}. \tag{10b}$$

This same vertical difference in neutral density is also related to the vertical difference in pressure on the reference cast by (this follows simply from the definition of b)

$$[\ln \gamma^n]^D_A \approx -b\rho^{-1}g^{-2}N^2(p^A - p^D) \tag{10c}$$

and eliminating $(p^A - p^D)$ between (10b) and (10c) gives

$$[\ln \gamma^n]^D_A \approx -\frac{1}{2}bT_bF(\Theta - \Theta^r)\dot{p}\delta t \tag{10d}$$

where

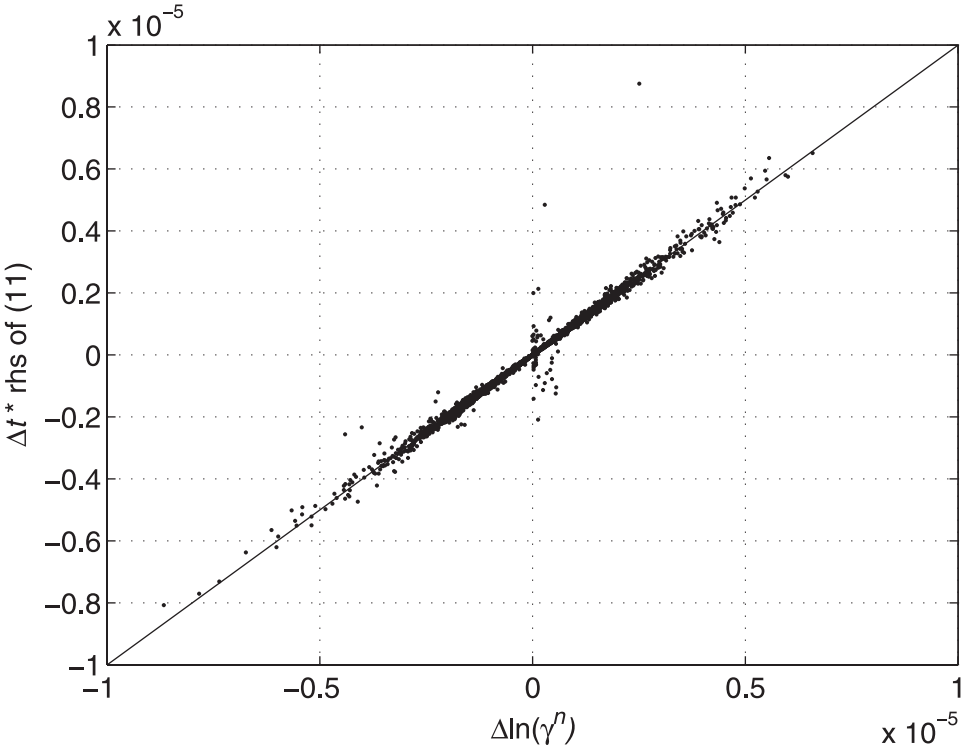

Figure 4. A scatter plot of the two sides of Eq. (11) which is an expression for the contribution of pressure changes to the material derivative of neutral density.

$$F = \left[1 + \frac{1}{2} T_b \rho g^2 N^{-2} \{ (\Theta - \Theta^r) - (p - p^r) \Theta_p^r \} \right]^{-1} \tag{10e}$$

and F is usually close to unity. Hence the contribution of $\dot{p}$ to the material derivative of neutral density is given by

$$\dot{p} \left. \frac{\partial \ln \gamma^n}{\partial p} \right|_{S,\Theta,x,y} \approx -b \frac{1}{2} T_b F (\Theta - \Theta^r) \dot{p}. \tag{11}$$

Figure 4 shows this contribution to the material derivative of neutral density due to changes in pressure. The two axes of the figure show respectively Δt times the two sides of (11) for a given pressure excursion Δp. A random $\{S_0, T_0, p_0, \gamma_0^n, \text{long}, \text{lat}\}$ observation from the labeled Levitus data set is initially perturbed randomly in T and pressure p, and then deterministically in S in order to retain neutrality. The temperature excursions ΔT_0 correspond to conservative temperature excursions of up to ± 1°C at the sea surface and ± 0.1°C at the sea floor, with the conservative temperature limit being taken linearly in pressure between these extremes. Pressure perturbations Δp_0 up to ± 150 dbar are also imposed so that the random datum is well removed from the labeled data set. The salinity

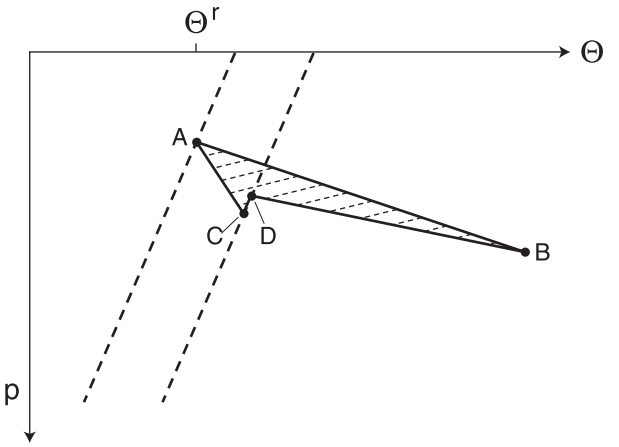

Figure 5. Conservative temperature-pressure plot of points A, B, and D along a neutral trajectory and point C on the same neutral density surface as A, that are used to deduce the contribution of horizontal advection to changes to the material derivative of neutral density.

excursion ΔS_0 is then found that results in the observation $\{S_0 + \Delta S_0, T_0 + \Delta T_0, p_0 + \Delta p_0$, long, lat$\}$ having the neutral density value γ_0^n and this becomes the initial random observation $\{S, T, p$, long, lat$\}$ lying remote to the labeled Levitus cast for which we calculate the contribution to the material derivative given by (11). Values for b, T_b and Θ^r are all found at the initial location $\{S_0, T_0, p_0, \gamma_0^n$, long, lat$\}$ on the labeled Levitus cast, since this is the point of intersection of the neutral density algorithm with the labeled data set.

The observation $\{S, T, p$, long, lat$\} = \{S_0 + \Delta S_0, T_0 + \Delta T_0, p_0 + \Delta p_0$, long, lat$\}$ is now perturbed randomly by a pressure increment Δp between -200 dbar and $+200$ dbar and then relabeled with neutral density γ^n. The location of the intersection of the γ^n surface with the labeled Levitus cast is used to calculate values of b, T_b, N^2 and Θ^r at this new intersection. These are then averaged with the values previously obtained to allow calculation of the right hand side of (11). The left-hand side is computed from the differences in the two γ^n labels assigned by the two calls to the neutral density algorithm. It is clear from Figure 4, where the results of 2×10^4 random calculations are plotted, that Eq. (11) holds to an excellent approximation. The correlation coefficient between the two axes is 0.995, confirming the veracity of (11).

5. The material derivative of neutral density caused by lateral advection

Now we consider the effect on $d \ln \gamma^n/dt$ of lateral advection of a fluid parcel without change in the parcel's S, Θ or p. The fluid parcel (S, Θ, p) at point B in Figure 5 communicates neutrally with the parcel A, (S^r, Θ^r, p^r), on the labeled reference cast at (x, y). When the fluid parcel B has moved to its new horizontal location at $(x + u\delta t, y + v\delta t)$ it retains its three properties (S, Θ, p) and communicates neutrally with parcel D on a

different pre-labeled reference cast, namely the reference cast at the new latitude and longitude, and bottle B is now given the neutral density label of point D. On this same reference cast, point C has the same pre-labeled value of neutral density as point A on the original reference cast at (x, y). The difference between the conservative temperature and pressure of bottles C and A is $\delta t \mathbf{V} \cdot \nabla_\gamma \Theta^r$ and $\delta t \mathbf{V} \cdot \nabla_\gamma p^r$. While points A and C both have the same value of neutral density, it is not 100% accurate to say that these parcels are neutrally related as parcels would be on a neutral trajectory. This is because the small values of helicity in the ocean ensure that any well-defined surface such as a neutral density surface cannot be completely neutral (McDougall and Jackett, 1988; 2005a). The difference in slope between a neutral density surface and the local neutral tangent plane has been shown to be very small in the labeled Levitus atlas data of the neutral density algorithm (see Jackett and McDougall (1997), McDougall and Jackett (2005b), the curve labeled "γ^n (labeled Levitus)" in Fig. 11 below, and the right-hand most bar in Fig. 12). We proceed with the approximation that takes points A and C to be neutrally related and we will subsequently make a correction for this approximation.

Now consider the trajectory C-A-B-D. The first of these three legs can be considered to be a neutral trajectory and the other two legs are both neutral trajectories. Hence, as in the previous section, the closed integral on the $\Theta - p$ diagram gives the difference between the locally referenced potential density of parcels D and C

$$(\rho_\Theta^D - \rho_\Theta^C)/\rho_\Theta \approx \oint T_b [p - p^r] d\Theta \tag{12}$$

where the closed shaded area is enclosed by the straight lines C-A-B-D-C and the potential density is referenced to $p^r = (p^D + p^C)/2$. This area on Figure 5 is the difference of the areas of the two triangles CAB and CDB. The triangle CAB has lengths $(\Theta - \Theta^r)$ in the Θ direction and $\{\mathbf{V} \cdot \nabla_\gamma p^r - \mathbf{V} \cdot \nabla_\gamma \Theta^r (p - p^r)/(\Theta - \Theta^r)\}$ in the p direction, while the triangle CDB has the same length $(\Theta - \Theta^r)$ in the Θ direction while the length in the p direction is proportional to $(p^C - p^D)$ such that the area of triangle CDB is $\frac{1}{2}(p^C - p^D)\{(\Theta - \Theta^r) - (p - p^r)\Theta_p^r\}$. Taking the difference of the areas of these triangles leads to

$$\begin{aligned}[\ln \gamma^n]_C^D \approx & -\frac{1}{2} b T_b \{(\Theta - \Theta^r)\mathbf{V} \cdot \nabla_\gamma p^r - (p - p^r)\mathbf{V} \cdot \nabla_\gamma \Theta^r\} \delta t \\ & + \frac{1}{2} b T_b (p^C - p^D)\{(\Theta - \Theta^r) - (p - p^r)\Theta_p^r\}.\end{aligned} \tag{12a}$$

Similarly to (10c) we note that the vertical difference of neutral density between points C and D is given by

$$[\ln \gamma^n]_C^D \approx -b \rho^{-1} g^{-2} N^2 (p^C - p^D) \tag{12b}$$

and eliminating $(p^C - p^D)$ between (12a) and (12b) gives

$$[\ln \gamma^n]_A^D \approx -\frac{1}{2} bT_b F\{(\Theta - \Theta^r)\mathbf{V} \cdot \nabla_\gamma p^r - (p - p^r)\mathbf{V} \cdot \nabla_\gamma \Theta^r\}\delta t \tag{13}$$

where F is given as before by (10e). Hence the contribution of lateral advection to the material derivative of neutral density is

$$u \left.\frac{\partial \ln \gamma^n}{\partial x}\right|_{S,\Theta,p,y} + v \left.\frac{\partial \ln \gamma^n}{\partial y}\right|_{S,\Theta,p,x} \approx -\frac{1}{2} bT_b F\{(\Theta - \Theta^r)\mathbf{V} \cdot \nabla_\gamma p^r - (p - p^r)\mathbf{V} \cdot \nabla_\gamma \Theta^r\}. \tag{14a}$$

This relationship has been checked in a similar manner to the checking of relationship (11) of the previous section. Random neutral excursions $\{S_0 + \Delta S_0,\ T_0 + \Delta T_0,\ p_0 + \Delta p_0,$ long, lat$\}$ are taken from random observations $\{S_0,\ T_0,\ p_0,\ \gamma_0^n,$ long, lat$\}$ in the labeled Levitus data set. The maximum temperature and pressure perturbations, ΔT_0 and Δp_0, are the same as in the previous section, and the salinity perturbation ΔS_0 is again taken so that $\{S_0 + \Delta S_0,\ T_0 + \Delta T_0, p_0 + \Delta p_0,$ long, lat$\}$ has neutral density γ_0^n. As in the previous section, values for b, T_b, Θ^r and p^r are all found at the initial location $\{S_0, T_0, p_0,$ γ, long, lat$\}$ on the labeled Levitus cast. Next we increment longitude and latitude each by one degree and re-label this datum by finding the points of intersection of the neutral tangent plane with the labeled Levitus data. This time however there are four points of intersection with the labeled data set, since the longitude and latitude of the perturbed observation $\{S_0 + \Delta S_0, T_0 + \Delta T_0, p_0 + \Delta p_0,$ long $+ 1,$ lat $+ 1\}$ places the datum strictly inside one of the boxes of the labeled data set. Values for b, T_b, Θ^r and p^r are thus weighted averages of the values of these same quantities at each of the four casts of the labeled data set surrounding the laterally perturbed observation. These are now averaged with the prior values of b, T_b, Θ^r and p^r, resulting in an estimate of Δt times the right-hand side of (14a). The left-hand side of (14a), multiplied by Δt, is calculated from the differences of the natural logarithms of the two different values of γ^n returned by the neutral density code. Figure 6 shows these two quantities on the two axes for 2×10^4 random calculations, where the approximate balance of (14a) is obvious. The correlation coefficient of the two axes is 0.94 confirming the veracity of (14a).

The development (12)–(14a) has assumed both that parcels A and C are neutrally related and that these parcels in the reference data set have the same neutral density. As mentioned above, along a neutral trajectory in the reference data set there will be a small variation in neutral density so that to (14a) should be added the lateral advection $\mathbf{V} \cdot \nabla_n \ln \gamma^n|^r$ of neutral density along the neutral tangent plane in the reference data set. The difference in slope between the neutral tangent plane and the neutral density surface in the labeled reference data set is

$$\mathbf{s} \equiv \nabla_n z^r - \nabla_\gamma z^r \tag{14b}$$

and this can also be expressed (see McDougall and Jackett, 1988) as $-gN^{-2}(\alpha \nabla_\gamma \Theta^r - \beta \nabla_\gamma S^r)$ which illustrates the fact that the gradients of temperature and salinity are not quite

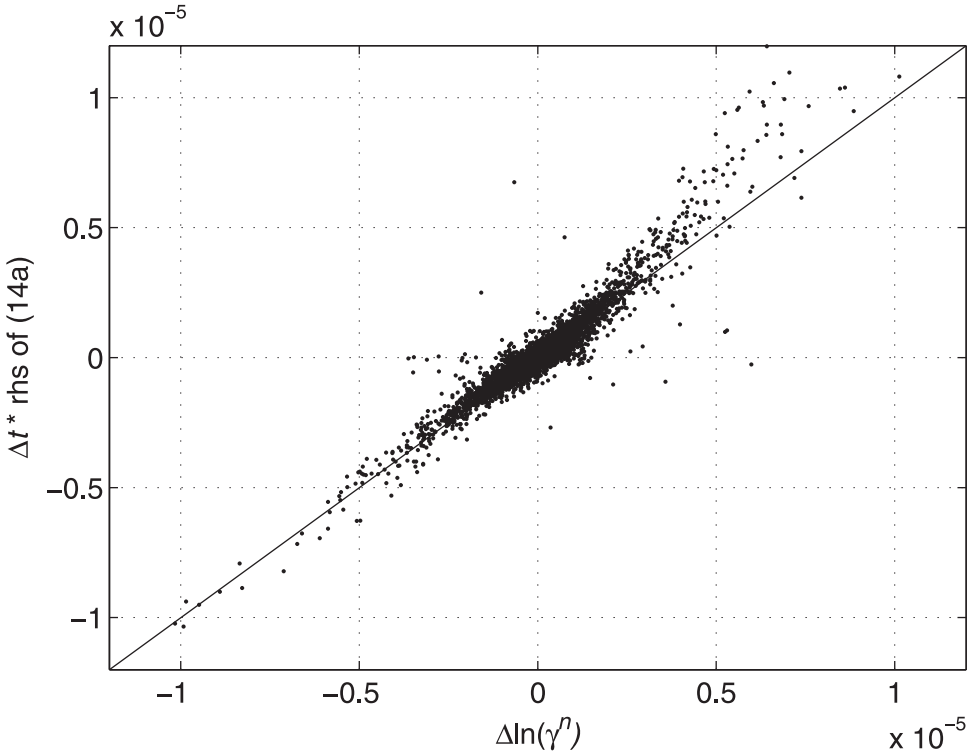

Figure 6. A scatter plot of the two sides of Eq. (14a) which is an expression for the contribution of horizontal advection to the material derivative of neutral density.

density compensated along the neutral density surface. The extra contribution to the lateral advection of the logarithm of neutral density by this difference in slope **s** is then $-bg^{-1}N^2\mathbf{V}\cdot\mathbf{s}$ and this must be added to (14a) so that the total contribution of lateral advection to the material derivative of the logarithm of neutral density is

$$u\left.\frac{\partial \ln\gamma^n}{\partial x}\right|_{S,\Theta,p,y} + v\left.\frac{\partial \ln\gamma^n}{\partial y}\right|_{S,\Theta,p,x} \approx -\frac{1}{2}bT_bF\{(\Theta-\Theta^r)\mathbf{V}\cdot\nabla_\gamma p^r - (p-p^r)\mathbf{V}\cdot\nabla_\gamma\Theta^r\} - bg^{-1}N^2\mathbf{V}\cdot\mathbf{s}. \tag{14c}$$

6. The material derivative of neutral density caused by irreversible mixing

Now we allow irreversible mixing processes to alter the salinity and conservative temperature of our initial parcel B, taking its properties from (S^B, Θ^B, p^B) to $(S^B + \dot{S}\delta t, \Theta^B + \dot{\Theta}\delta t, p^B)$ while remaining at constant pressure, latitude and longitude. The original parcel B is connected neutrally to the "bottle" (S^A, Θ^A, p^A) on the labeled reference cast at (x, y). That is, the two fluid parcels A and B both have the same density when referenced

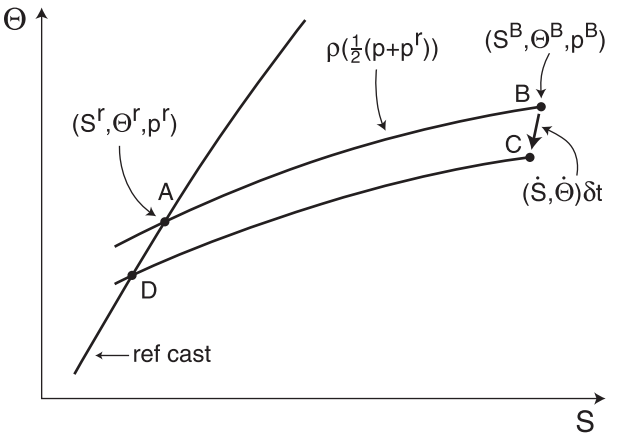

Figure 7. Salinity-conservative temperature plot of points A and B that are neutrally related, and points C and D that are also neutrally related. This diagram is used to develop the contribution of irreversible mixing to the material derivative of neutral density.

to the mean pressure, $\bar{p} = 0.5(p^A + p^B)$, as in Figure 7. The modified parcel B, namely $(S^B + \dot{S}\delta t,\ \Theta^B + \dot{\Theta}\delta t,\ p^B)$ will be connected neutrally to a different fluid parcel (not shown) on the reference cast.

In order to make progress we split the derivation into two parts. First we consider a parcel C that has the updated salinity and conservative temperature of parcel B, but has a different pressure, so chosen that the average pressure of parcel C and the parcel on the reference cast which talks neutrally to it, parcel D, is the same as $\bar{p} = 0.5(p^A + p^B)$. That is, parcels C and D have the properties $(S^B + \dot{S}\delta t,\ \Theta^B + \dot{\Theta}\delta t,\ p^B - \delta p)$ and $(S^D,\ \Theta^D,\ p^A + \delta p)$ and they both have the same value of potential density referenced to $\bar{p} = 0.5(p^A + p^B) = 0.5(p^C + p^D)$. The pressure perturbation δp remains to be determined. The change in this potential density caused by the material derivatives of S and Θ for parcel C is

$$d \ln \rho_\Theta(\bar{p})/dt = \beta(\bar{p})\dot{S} - a(\bar{p})\dot{\Theta} \tag{15}$$

and this change in potential density is evident in Figure 7 as both the differences between parcels B and C and between parcels A and D. In order to relate these changes in potential density to changes in neutral density on the reference cast, we first evaluate the difference in locally-referenced potential density on the reference cast. The logarithmic vertical gradient of this locally referenced potential density at $p^r = p^A$ is the vertical gradient of $\ln \rho_\Theta(\bar{p})$ times $\{a(p^r)\Theta^r_z - \beta(p^r)S^r_z\}/\{a(\bar{p})\Theta^r_z - \beta(\bar{p})S^r_z\}$, so that for parcel C

$$d \ln \rho_\Theta(p^r)/dt = (\beta(\bar{p})\dot{S} - a(\bar{p})\dot{\Theta})\{a(p^r)\Theta^r_z - \beta(p^r)S^r_z\}/\{a(\bar{p})\Theta^r_z - \beta(\bar{p})S^r_z\}. \tag{16}$$

By definition, the vertical gradient of the logarithm of neutral density is b times the vertical gradient of the logarithm of locally-referenced potential density (Jackett and McDougall,

1997), so the contribution of irreversible mixing to the material derivative of neutral density for parcel C is simply b times (16), namely

$$b(\beta(\bar{p})\dot{S} - a(\bar{p})\dot{\Theta})(a(p^r)\Theta_z^r - \beta(p^r)S_z^r)/(a(\bar{p})\Theta_z^r - \beta(\bar{p})S_z^r)$$
$$\approx b(\beta(\bar{p})\dot{S} - a(\bar{p})\dot{\Theta})\left(1 - (1 - R_\rho^{-1})^{-1}\frac{1}{2}\alpha^{-1}T_b(p - p^r)\right) \tag{17}$$

where the second line represents the first two terms in powers of $(p - p^r)$ in a Taylor series expansion where the pressure variation of β has also been ignored in comparison to that of α, and R_ρ is the vertical stability ratio of the water column at the reference cast, $R_\rho = \alpha(p^r)\Theta_z^r/(\beta(p^r)S_z^r)$.

We are not yet done in this section because parcel C has an unwanted change in pressure, and this needs to be countered using the result (11) of Section 4. The vertical distance between the two points A and D on the reference cast, is given by δt times (15) divided by $(\beta(\bar{p})S_z^r - \alpha(\bar{p})\Theta_z^r)$, and the pressure difference, $p^D - p^A$, divided by the time interval δt is the value of $\dot{p}$ that must be added to parcel C to retain the pressure of the sum of the two processes constant at p^B. Using this value of $\dot{p}$ in the expression (11) shows that the additional contribution to the material derivative of neutral density is

$$\frac{1}{2}\rho g b T_b F(\Theta - \Theta^r)(\alpha(\bar{p})\dot{\Theta} - \beta(\bar{p})\dot{S})/(\alpha(\bar{p})\Theta_z^r - \beta(\bar{p})S_z^r) \tag{18}$$

where F is again given by (10e). The sum of the contributions of these two processes is the material rate of change of neutral density at fixed values of pressure, latitude and longitude, which is simply the following sum of (17) and (18), (noting that the square of the buoyancy frequency N on the reference cast is given by $g(a(p^r)\Theta_z^r - \beta(p^r)S_z^r)$)

$$\dot{S}\left.\frac{\partial \ln \gamma^n}{\partial S}\right|_{\Theta,p,x,y} + \dot{\Theta}\left.\frac{\partial \ln \gamma^n}{\partial \Theta}\right|_{S,p,x,y} \approx -bg^{-1}\frac{(a(\bar{p})\dot{\Theta} - \beta(\bar{p})\dot{S})}{(a(\bar{p})\Theta_z^r - \beta(\bar{p})S_z^r)}\left(N^2 - \frac{1}{2}\rho g^2 T_b F(\Theta - \Theta^r)\right) \tag{19}$$

$$\approx -b(a(\bar{p})\dot{\Theta} - \beta(\bar{p})\dot{S})\left(1 - (1 - R_\rho^{-1})^{-1}\frac{1}{2}\alpha^{-1}T_b(p - p^r)\right)\left(1 - \frac{1}{2}\rho g^2 N^{-2} T_b F(\Theta - \Theta^r)\right).$$

The first line of the right-hand side of (19) has been checked using a similar finite difference technique to the checks of (11) and (14a) in the previous two sections. Random neutral excursions $\{S_0 + \Delta S_0, T_0 + \Delta T_0, p_0 + \Delta p_0, \text{long}, \text{lat}\}$ are taken from random observations $\{S_0, T_0, p_0, \gamma_0^n, \text{long}, \text{lat}\}$ in the labeled Levitus data set, with the maximum temperature and pressure perturbations ΔT_0 and Δp_0 being the same as before. The salinity perturbation ΔS_0 is taken to ensure neutrality, in terms of lying on the same neutral tangent plane so that $\{S_0 + \Delta S_0, T_0 + \Delta T_0, p_0 + \Delta p_0, \text{long}, \text{lat}\}$ has the same neutral density as $\{S_0, T_0, p_0, \gamma_0^n, \text{long}, \text{lat}\}$. Values for b, T_b, ρ, N^2, Θ^r, S_z^r and Θ_z^r are all found at the initial location $\{S_0, T_0, p_0, \gamma_0^n, \text{long}, \text{lat}\}$ on the labeled Levitus cast, while the mid-pressure coefficients are computed as $\alpha(S_0, T_0, \bar{p})$ and $\beta(S_0, T_0, \bar{p})$ where $\bar{p} = (p_0 +$

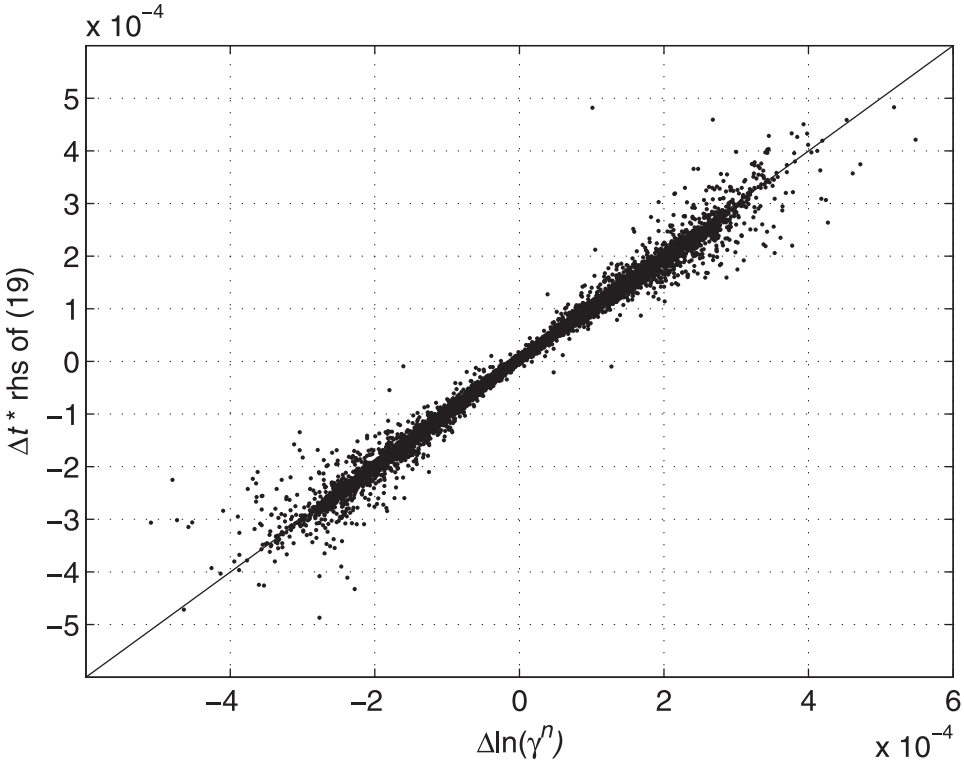

Figure 8. A scatter plot of the two sides of Eq. (19) which is an expression for the contribution of irreversible mixing to the material derivative of neutral density.

$p)/2$. The observation $\{S, T, p, \text{long, lat}\} = \{S_0 + \Delta S_0, T_0 + \Delta T_0, p_0 + \Delta p_0, \text{long, lat}\}$ is now perturbed by random salinity and temperature perturbations in the range between -0.2 psu and $+0.2$ psu and in the range between -1.0°C and $+1.0$°C and then $\{S + \Delta S, T + \Delta T, p, \text{long, lat}\}$ is re-labeled with neutral density and the intersection $\{S_1, T_1, p_1, \gamma, \text{long, lat}\}$ of the neutral tangent plane with the labeled Levitus cast is used to compute new values of b, T_b, ρ, N^2, Θ^r, S_z^r and Θ_z^r, and mid-pressure values $\alpha(S_1, T_1, \bar{p})$ and $\beta(S_1, T_1, \bar{p})$, where now $\bar{p} = (p_1 + p)/2$. These two sets of cast and mid-pressure values are averaged and then used to calculate Δt times the right-hand side of (19). This is plotted in Figure 8 against Δt times the left-hand side of (19), namely $\Delta \ln(\gamma^n)$, for 2×10^4 random computations, where again we find good agreement between both sides of the equation. The correlation coefficient between the two axes is 0.994.

7. The dianeutral velocity

The material derivative of neutral density is then the sum of the three different effects, given by the sum of (11), (14c) and (19), namely

$$d\ln\gamma^n/dt \approx -b\frac{1}{2}T_bF(\Theta-\Theta^r)\dot{p} \tag{20}$$

$$-\,b\,\frac{1}{2}T_bF\{(\Theta-\Theta^r)\mathbf{V}\cdot\nabla_\gamma p^r-(p-p^r)\mathbf{V}\cdot\nabla_\gamma\Theta^r\}$$

$$-\,bg^{-1}N^2\mathbf{V}\cdot\mathbf{s}$$

$$-\,b\left(g^{-1}N^2-\frac{1}{2}\rho gT_bF(\Theta-\Theta^r)\right)\frac{(a(\bar{p})\dot{\Theta}-\beta(\bar{p})\dot{S})}{(a(\bar{p})\Theta^r_z-\beta(\bar{p})S^r_z)}.$$

The last line here is to be expected in the sense that when there are diabatic mixing processes, so that $\dot{\Theta}$ and $\dot{S}$ are nonzero, one would expect that neutral density would change. The first line says that when there is a water mass contrast between the fluid parcel and the labeled reference cast (from whence the parcel gains its neutral density label) then any changes in the pressure of the fluid parcel, including those changes due to adiabatic and isohaline movements, lead to changes in the parcel's neutral density. Note that the temperature contrast is a local contrast in the sense that it does not involve the total variation of water masses over the whole world ocean but only the change in water mass with time (eg seasonal changes) at a given horizontal location. The second line in (20) is nonzero if the ratio of $\mathbf{V}\cdot\nabla_\gamma p^r$ and $\mathbf{V}\cdot\nabla_\gamma\Theta^r$ is not the same as the ratio of $(p-p^r)$ to $(\Theta-\Theta^r)$. This term scales the same as the first term on the right of (20) in that $\dot{p}$ and $\mathbf{V}\cdot\nabla_\gamma p^r$ tend to have similar magnitudes.

Writing the material derivative of pressure with respect to neutral density coordinates,

$$\dot{p} = p_t\big|_\gamma + \mathbf{V}\cdot\nabla_\gamma p + e^\gamma p_z, \tag{21}$$

where e^γ is the vertical velocity through the neutral density surface (called dianeutral velocity for convenience) we write the left-hand side of (20) as $e^\gamma(\ln\gamma^n)_z$, and follow de Szoeke *et al.* (2000) in collecting the terms in e^γ together so that (20) becomes

$$e^\gamma \approx (\psi^\gamma-1)(p_t\big|_\gamma+\mathbf{V}\cdot\nabla_\gamma p)(p_z)^{-1} \tag{22}$$

$$+\,(\psi^\gamma-1)\left(\mathbf{V}\cdot\nabla_\gamma p^r-\frac{(p-p^r)}{(\Theta-\Theta^r)}\mathbf{V}\cdot\nabla_\gamma\Theta^r\right)(p_z)^{-1}$$

$$+\,\psi^\gamma\mathbf{V}\cdot\mathbf{s}$$

$$+\,(\psi^\gamma+(\psi^\gamma-1))\frac{(a(\bar{p})\dot{\Theta}-\beta(\bar{p})\dot{S})}{(a(\bar{p})\Theta^r_z-\beta(\bar{p})S^r_z)}$$

where ψ^γ is defined by

$$\psi^\gamma = \frac{\left[N^2+\frac{1}{2}\rho g^2T_b(\Theta-\Theta^r)-\frac{1}{2}\rho g^2T_b(p-p^r)\Theta^r_p\right]}{\left[N^2+\rho g^2T_b(\Theta-\Theta^r)-\frac{1}{2}\rho g^2T_b(p-p^r)\Theta^r_p\right]} \tag{23a}$$

so that $(\psi^\gamma - 1)$ is

$$(\psi^\gamma - 1) = \frac{-\frac{1}{2}\rho g^2 T_b(\Theta - \Theta^r)}{\left[N^2 + \rho g^2 T_b(\Theta - \Theta^r) - \frac{1}{2}\rho g^2 T_b(p - p^r)\Theta_p^r\right]}. \tag{23b}$$

Hence $(\psi^\gamma - 1)$ is nonzero to the extent that there is a water mass contrast $(\Theta - \Theta^r)$ between the seawater parcel that is being labeled and the data on the labeled reference data set that communicates neutrally with the seawater sample. For reasonable values of $(\Theta - \Theta^r)$ and $(p - p^r)$ the denominator in (23a) and (23b) is close to N^2 and ψ^γ is close to 1.

Eqs. (20) and (22) are the main results of this paper so far, being expressions for the material derivative of neutral density and the dianeutral velocity. The form (22) is useful as it isolates the undesirable feature that the vertical velocity through a neutral density surface is not only caused by irreversible mixing processes, but also is partially due to adiabatic motions such as the vertical heave of the water column. The first three lines of (22) represent the contribution to the flow through the neutral density surface of (i) the adiabatic temporal heaving of the neutral density surface, (ii) the adiabatic sliding of fluid along the neutral density surface, and (iii) the fact that neutral tangent planes do not exactly coincide with neutral density surfaces even in the reference data set. Note that as $(\Theta - \Theta^r)$ tends to zero, $(\psi^\gamma - 1)$ also tends to zero so that the second line of (22) is well-behaved and becomes proportional to $(p - p^r)\mathbf{V} \cdot \nabla_\gamma \Theta^r$.

8. Neutral limitations of $\gamma^a(S, \Theta)$

We consider now how neutral a function of only S and Θ, $\gamma^a(S, \Theta)$, can be. We ask what feature of the ocean hydrography limits the ability to achieve a minimum or zero value of the gradient of γ^a everywhere in a neutral tangent plane, $\nabla_n \gamma^a$? We can write $\nabla_n \gamma^a$ as

$$\nabla_n \gamma^a = b(S, \Theta)\nabla_n S - a(S, \Theta)\nabla_n \Theta \tag{24}$$

where $b(S, \Theta) = \gamma_S^a$ and $a(S, \Theta) = -\gamma_\Theta^a$. Since $\beta(S, \Theta, p)\nabla_n S = \alpha(S, \Theta, p)\nabla_n \Theta$ in a neutral tangent plane, (24) can be written as

$$a^{-1}\nabla_n \gamma^a = \nabla_n \Theta \left\{ \frac{b(S, \Theta)}{a(S, \Theta)} \frac{\alpha(S, \Theta, p)}{\beta(S, \Theta, p)} - 1 \right\}. \tag{25}$$

If pressure is a single-valued function of temperature along a neutral trajectory, then it is clearly possible to choose the functions $a(S, \Theta)$ and $b(S, \Theta)$ such that their ratio is equal to $(\alpha/\beta)(S, \Theta, p)$ and hence $\nabla_n \gamma^a = \mathbf{0}$. If, however, $p(\Theta)$ ceases to be a single-valued function along the neutral trajectory such as at the point marked with a cross in Figure 9, then it becomes impossible to maintain $\nabla_n \gamma^a = \mathbf{0}$. To see this we pursue a reductio ad absurdum proof by assuming $\nabla_n \gamma^a = \mathbf{0}$, and then consider two points, say points 1 and 2, that have the same value of Θ on either side of the extremum in Θ. Since $b(S, \Theta)$ is the

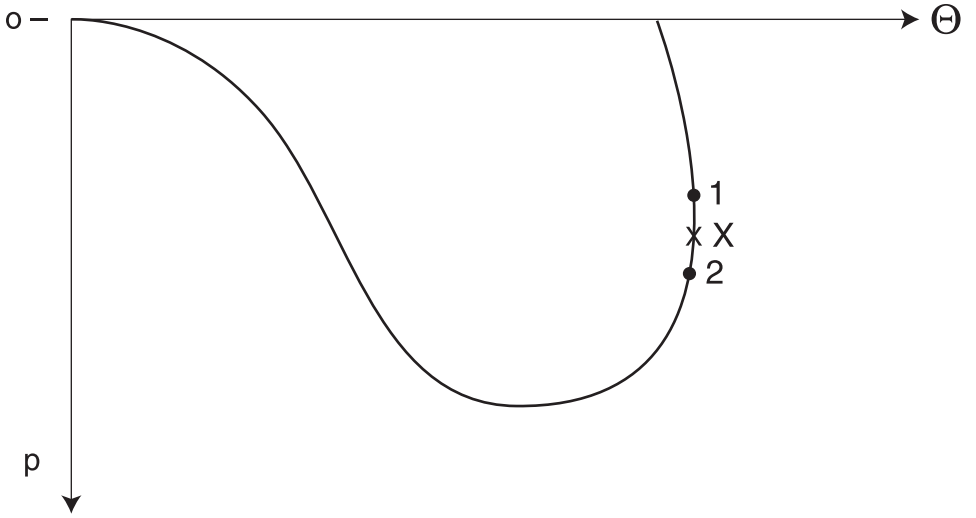

Figure 9. Sketch of the variation of conservative temperature and pressure along a neutral trajectory from the southern to the northern hemisphere. The discussion in the text concentrates on the point of extreme temperature on this diagram, marked with a cross.

saline contraction coefficient for the approximate density variable, we require it to be nonzero, implying that S can be written as a function of γ^a and Θ. Hence the two parcels have not only the same values of Θ and γ^a but also the same values of salinity. However, since the two parcels have different pressures, $(\alpha/\beta)(S, \Theta, p)$ is different on either side of the temperature extremum so that (from (25)) $\nabla_n \gamma^a$ cannot be zero all the way from point 1 to point 2 along the neutral trajectory, contradicting the assumption that $\nabla_n \gamma^a = \mathbf{0}$. We conclude that it is the multi-valued nature of $p(\Theta)$ in Figure 9; that is, the fact that p is not a single-valued function of Θ along the neutral trajectory that ensures that any and every variable that is a function only of S and Θ must vary along the neutral trajectory.

We can also understand this inherent limitation to the neutrality of a function of S and Θ by considering the region in space near a location where $\nabla S \times \nabla\Theta = \mathbf{0}$ as shown in Figure 10. The surfaces of constant salinity and temperature will in general have different curvatures in space and we show two locations marked A and B which have the same values of S and Θ. In general these isohaline and isothermal surfaces will not be flat but rather they will have a gradient of pressure along them so that parcels A and B will have different values of p. Hence the pressures of these two parcels cannot both be described by the same single-valued function $p = p(S, \Theta)$. Without a single functional form $p = p(S, \Theta)$ it is not possible to choose any function $\gamma^a(S, \Theta)$ so as to have (25) being zero. We conclude that it is from locations where $\nabla S \times \nabla\Theta = \mathbf{0}$ that the different branches of $p = p(S, \Theta)$ diverge. In other words, different branches of this function emanate from locations where $\nabla_n \Theta = \mathbf{0}$ and $\nabla_n p \neq \mathbf{0}$, and it is these locations that ensure that $\gamma^a(S, \Theta)$ cannot be neutral.

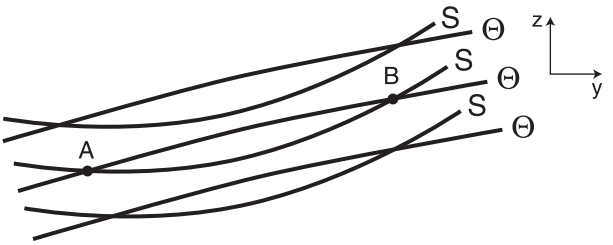

Figure 10. Sketch of some surfaces of constant S and of Θ surrounding the location where $\nabla S \times \nabla\Theta = \mathbf{0}$. Note the two points marked A and B that have the same values of S and Θ, but in general have different values of pressure. Hence the pressure at points A and B cannot both be described by the same function $p(S, \Theta)$.

9. Approximate forms of neutral density, $\gamma^a(S, \theta)$ and $\gamma^a(S, \Theta)$

We seek two approximate functions for neutral density γ^n when expressed in terms of salinity S and either potential temperature θ or conservative temperature Θ. The functional form adopted for both of these functions is a rational function, i.e., a ratio of two polynomials. Recent work with the equation of state in McDougall *et al.* (2003) and Jackett *et al.* (2005) has found advantages in these approximating functions over more traditional polynomials. These advantages relate to the numerical stability of the functional form, the economy of its computational cost and the ability of this form in approximating a larger class of functions than those that can be accommodated by polynomials. The traditional equation of state, known as the International Equation of State (Fofonoff and Millard, 1983) also possesses this structure.

The exact form for the rational functions is that suggested by the fits to the equation of state in McDougall *et al.* (2003) and Jackett *et al.* (2005). Specifically, for just two independent variables S and one of either θ or Θ, this reduces to a rational function with a numerator of 7 terms and a denominator with 10 terms, for a total of 16 unknown parameters. The precise definitions of these functions are

$$\gamma^a(S, \theta) = \frac{P_n(S, \theta)}{P_d(S, \theta)} \qquad \text{and} \qquad \gamma^a(S, \Theta) = \frac{P_n(S, \Theta)}{P_d(S, \Theta)}, \tag{26}$$

where the terms and coefficients of $P_n(S, \theta)$, $P_d(S, \theta)$, $P_n(S, \Theta)$, and $P_d(S, \Theta)$ are given in Tables 1 and 2. The coefficients have been computed by minimizing a cost function that is a weighted sum of several components that include: (i) the root mean squared difference between a global γ^n field and the corresponding rational function approximation, (ii) the maximum absolute difference between the global γ^n field and the corresponding rational function approximation and (iii) the percentage of the global ocean whose fictitious diapycnal diffusivity $D^{\text{fictitious}} = K|\nabla_{\gamma^a} z - \nabla_n z|^2$ exceeds 10^{-5} m^2 s^{-1}. Here ∇_{γ^a} and ∇_n are respectively the two dimensional lateral gradient operators in the approximating rational function surface and the well defined neutral tangent plane, and K is a lateral diffusivity, which we take as 1000 m^2 s^{-1}. The quantity $K|\nabla_{\gamma^a} z - \nabla_n z|^2$ represents the diffusivity of density that is fluxed across the neutral tangent plane when the tangent of the

Table 1. Terms and coefficients of the polynomials $P_n(S, \theta)$ and $P_d(S, \theta)$ defining the rational function approximation of neutral density γ^n. A check value is $\gamma^a(35, 20) = 1024.59416751197$ kg m^{-3}.

$P_n(S, \theta)$	Coefficients	$P_d(S, \theta)$	Coefficients
constant	$1.0023063688892480 \times 10^{3}$	constant	1.0
θ	$2.2280832068441331 \times 10^{-1}$	θ	$4.3907692647825900 \times 10^{-5}$
θ^2	$8.1157118782170051 \times 10^{-2}$	θ^2	$7.8717799560577725 \times 10^{-5}$
θ^3	$-4.3159255086706703 \times 10^{-4}$	θ^3	$-1.6212552470310961 \times 10^{-7}$
S	$-1.0304537539692924 \times 10^{-4}$	θ^4	$-2.3850178558212048 \times 10^{-9}$
$S\theta$	$-3.1710675488863952 \times 10^{-3}$	S	$-5.1268124398160734 \times 10^{-4}$
S^2	$-1.7052298331414675 \times 10^{-7}$	$S\theta$	$6.0399864718597388 \times 10^{-6}$
		$S\theta^3$	$-2.2744455733317707 \times 10^{-9}$
		$S^{3/2}$	$-3.6138532339703262 \times 10^{-5}$
		$S^{3/2}\theta^2$	$-1.3409379420216683 \times 10^{-9}$

surface corresponding to the approximating rational function does not line up exactly with this plane (see McDougall and Jackett, 2005b). The global γ^n field is obtained by labeling with neutral density the global atlas data of Gouretski and Koltermann (2004) (see also Koltermann *et al.,* 2004). Components (i) and (ii) fit the approximating rational functions to the neutral density variable γ^n, with component (ii) being necessary to achieve a monotonically increasing function of depth. Component (iii) minimizes the alignment of the approximating function with the neutral tangent plane, and is an important measure of the accuracy of any surface in such an approximation. Weights were chosen subjectively so as to achieve the best overall fits.

Figure 11 displays the frequency distribution of the logarithm to the base 10 of the fictitious diffusivity $D^{\text{fictitious}} = 1000|\nabla_{\text{Surface}} z - \nabla_n z|^2$ for various surfaces for all data in a global ocean atlas excluding the Arctic Ocean and marginal seas. The fictitious diapycnal diffusivity was evaluated for lateral mixing along γ^n surfaces, σ_2 surfaces and the

Table 2. Terms and coefficients of the polynomials $P_n(S, \Theta)$ and $P_d(S, \Theta)$ defining the rational function approximation of neutral density γ^n. A check value is $\gamma^a(35\text{-}20) = 1024.43863927763$ kg m^{-3}.

$P_n(S, \Theta)$	Coefficients	$P_d(S, \Theta)$	Coefficients
constant	$1.0022048243661291 \times 10^{3}$	constant	1.0
Θ	$2.0634684367767725 \times 10^{-1}$	Θ	$4.4946117492521496 \times 10^{-5}$
Θ^2	$8.0483030880783291 \times 10^{-2}$	Θ^2	$7.9275128750339643 \times 10^{-5}$
Θ^3	$-3.6670094757260206 \times 10^{-4}$	Θ^3	$-1.2358702241599250 \times 10^{-7}$
S	$-1.4602011474139313 \times 10^{-3}$	Θ^4	$-4.1775515358142458 \times 10^{-9}$
$S\Theta$	$-2.5860953752447594 \times 10^{-3}$	S	$-4.3024523119324234 \times 10^{-4}$
S^2	$-3.0498135030851449 \times 10^{-7}$	$S\Theta$	$6.3377762448794933 \times 10^{-6}$
		$S\Theta^3$	$-7.2640466666916413 \times 10^{-10}$
		$S^{3/2}$	$-5.1075068249838284 \times 10^{-5}$
		$S^{3/2}\Theta^2$	$-5.8104725917890170 \times 10^{-9}$

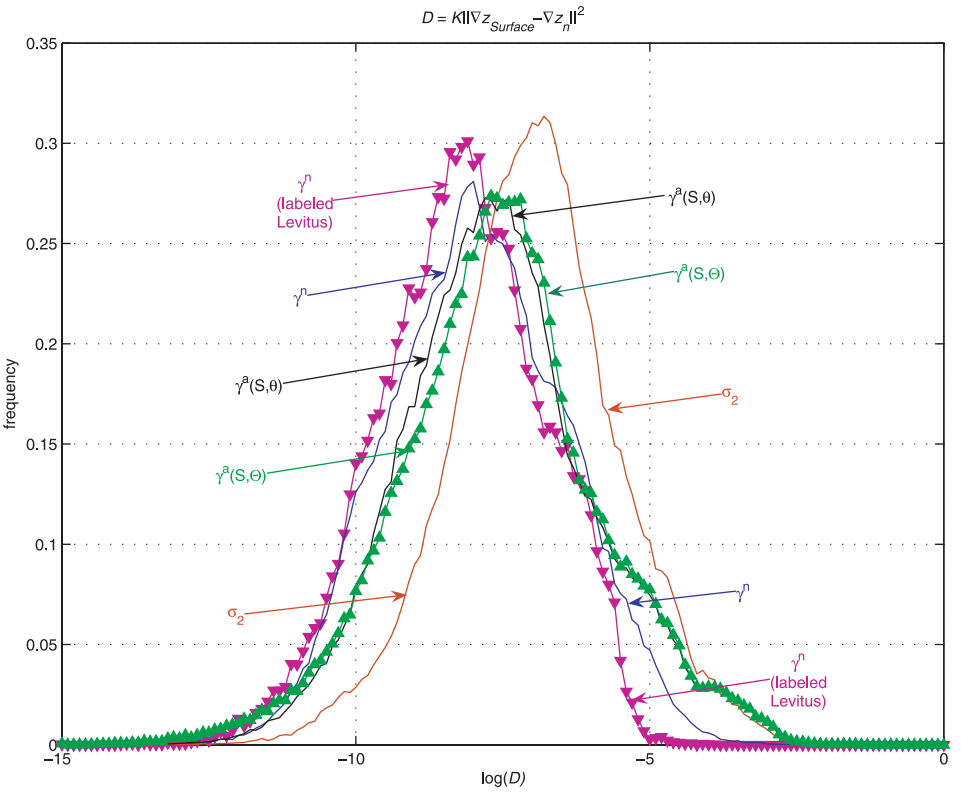

Figure 11. Frequency distribution of the logarithm of the fictitious diapycnal diffusivity arising from mixing along various coordinate surfaces.

iso-surfaces of the two rational functions $\gamma^a(S, \theta)$ and $\gamma^a(S, \Theta)$ of (26). The best surfaces in approximating the neutral tangent plane from this selection of surfaces are clearly the two neutral density surfaces. The more accurate one of these is the neutral density surface in the Levitus data that underlies the definition of neutral density; the computations for all other surfaces take place in the Gouretski and Koltermann (2004) global ocean atlas. The very small slope error when using the Levitus data set that is in the pre-labeled neutral density software indicates the inherent limitation in forming any kind of "density" surface due to the fact that neutral trajectories in the ocean are helical in nature. The σ_2 surface is more accurate than other potential density surfaces and orthobaric density surfaces (see McDougall and Jackett, (2005b)). The iso-surfaces corresponding to the two approximating rational functions lie in between the neutral density surfaces and the σ_2 surface, with the surfaces for the variables $\gamma^a(S, \Theta, p)$ and $\gamma^a(S, \theta, p)$ having very similar distributions.

In Figure 12 we show the percentage of data that has a fictitious diapycnal diffusivity larger than 10^{-5} m^2 s^{-1} for the five frequency distributions of Figure 11. It follows that in terms of this measure the two rational function approximations to neutral density yield surfaces that are better than the σ_2 surfaces, but are not as good as the surfaces of the full

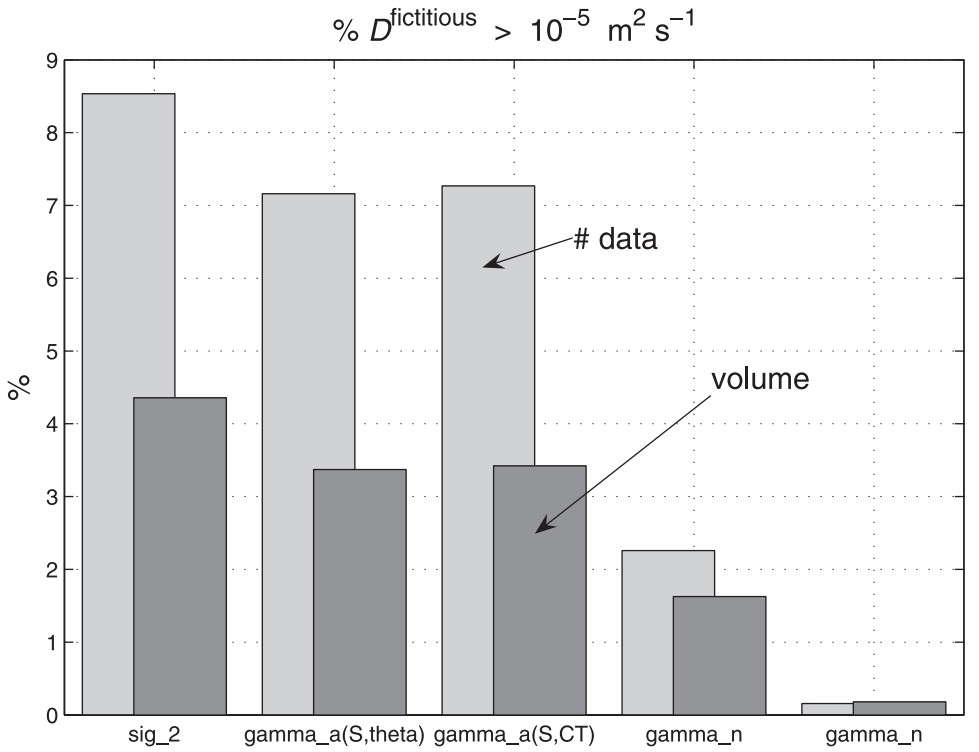

Figure 12. Percentages of the global ocean data for which the fictitious diapycnal diffusivity is greater than 10^{-5} m^2 s^{-1}. The right-hand bars are for the percentages of the global ocean volume while the left-hand bars are the percentages of data pairs in the global atlas (in which the standard pressures are more closely spaced in the upper ocean than in the deep).

neutral density variable. For example, in terms of the volume estimates, $\gamma^a(S, \theta)$ and $\gamma^a(S, \Theta)$ give improvements of 23% and 21% to the σ_2 estimate, compared to a 63% improvement for γ^n.

10. Discussion

We have argued that the low levels of mechanical energy dissipation in the ocean can be interpreted as providing evidence that the energetic mesoscale eddies do mix properties predominantly along the neutral tangent plane. This neutral tangent plane can be thought of locally as the potential density surface referenced to the pressure of the location in question. Section 3 above has demonstrated that the patched potential density method of Reid and Lynn (1971) locally approaches the neutral tangent plane in the limit as the intervals over which the patching procedure is applied is reduced towards zero.

Much of this paper has been spent deriving and verifying the expression (20) for the material derivative of neutral density (from which the expression (22) for the dianeutral velocity follows). The non-ideal nature of neutral density can be seen from (22) to be proportional to the expression (23b) for $(\psi^\gamma - 1)$ which is approximately proportional to

the water-mass contrast between the data in question and the reference cast of the pre-labeled data set to which the data are neutrally related. (In addition, there is the small term due to the ocean's helicity which means that even the reference data set of the neutral density software does not have neutral density surfaces exactly aligned with neutral tangent planes.) As the water-mass contrast ($\Theta - \Theta^r$) and the corresponding pressure difference ($p - p^r$) go to zero, so neutral density behaves as a quasi-material surface. The extent of the non quasi-material behavior is thus proportional to the contrasts in water-mass properties between the data and the local pre-labeled data. We use these expressions in McDougall and Jackett (2005b) to compare the extent of the non quasi-material nature of neutral density with that of orthobaric density.

The last part of this paper presents rational function approximations to neutral density, these rational functions being functions only of salinity and either potential temperature or conservative temperature (by contrast, neutral density also depends on pressure, latitude and longitude). Eden and Willebrand (1999) constructed such a variable just for the North Atlantic. They constrained their density variable to be not only as neutral as possible, but also so that its horizontal density gradient was as close as possible to the horizontal gradient of in situ density (which is equivalent to requiring that our factor b be close to unity). The rational functions presented here were derived with only one requirement in mind, namely to be as neutral as possible for a function of only the two conservative variables. These rational functions could be used to define the surfaces in a layered ocean model, using the technology developed by Sun *et al.* (1999) to evaluate the horizontal pressure gradient.

Acknowledgments. Our research on the meaning of "density surfaces" and the thermobaric terms in the equation of state relies on the tireless leadership of Nick Fofonoff over many years in improving the formulation of the equation of state, and we dedicate this research to his memory. We thank Dr Roland A. de Szoeke for his interest in quantifying the material derivative of neutral density which spurred us to do the work reported in Sections 4–7 of this paper. We also acknowledge that it was the skepticism expressed in de Szoeke *et al.* (2000) as to the neutrality of finely-patched potential density surfaces that led us to undertake the work described in Section 3. This work is a contribution to the CSIRO Climate Change Research Program.

APPENDIX

The variation of potential density in the neutral tangent plane

In the neutral tangent plane the gradients of salinity and conservative temperature are related neutrally so that (McDougall, 1987a)

$$\alpha(S, \Theta, p)\nabla_n\Theta = \beta(S, \Theta, p)\nabla_n S \tag{A1}$$

where α and β are the relevant thermal expansion and saline contraction coefficients. The gradient of potential density referenced to the general reference pressure p_r is given by

$$\nabla_n \ln \rho_\Theta = \beta(S, \Theta, p_r)\nabla_n S - \alpha(S, \Theta, p_r)\nabla_n\Theta = \beta(S, \Theta, p_r)\left[\frac{\alpha}{\beta}(p) - \frac{\alpha}{\beta}(p_r)\right]\nabla_n\Theta \tag{A2}$$

where the first expression simply comes from the chain rule of differentiation operating on

the functional form of potential density, $\rho_\Theta(S, \Theta, p_r)$, and the second expression has used (A1). Using the definition of the thermobaric parameter

$$T_b = \beta\partial(\alpha/\beta)/\partial p, \tag{A3}$$

to lowest order in the pressure difference $(p - p_r)$, (A2) can be written as

$$\nabla_n \ln \rho_\Theta \approx T_b[p - p_r]\nabla_n\Theta \tag{A4}$$

and in many applications the thermobaric parameter, $T_b \approx 2.7 \times 10^{-12}\ \mathrm{K}^{-1}\ \mathrm{Pa}^{-1}$, can be taken to be constant (see Fig. 9b of McDougall, 1987b).

REFERENCES

de Szoeke, R. A., S. R. Springer and D. M. Oxilia. 2000. Orthobaric density: A thermodynamic variable for ocean circulation studies. J. Phys. Oceanogr., *30,* 2830–2852.

Eden, C. and J. Willebrand. 1999. Neutral density revisited. Deep-Sea Res. II, *46,* 33–54.

Feistel, R. 2003. A new extended Gibbs thermodynamic potential of seawater. Prog. Oceanogr., *58,* 43–114.

Fofonoff, N. P. and R. C. Millard. 1983. Algorithms for computation of fundamental properties of seawater. UNESCO Technical Papers in Marine Science, *44,* UNESCO, 53 pp.

Gouretski, V. V. and K. P. Koltermann. 2004. WOCE Global Hydrographic Climatology. A Technical Report. Berichte des Bundesamtes für Seeschifffahrt und Hydrographie, *35,* 49 pp.

Griffies, S. M., A. Gnanadesikan, R. C. Pacanowski, V. D. Larichev, J. K. Dukowicz and R. D. Smith. 1998. Isoneutral diffusion in a z-coordinate ocean model. J. Phys. Oceanogr., *28,* 805–830.

Jackett, D. R. and T. J. McDougall. 1997. A neutral density variable for the world's oceans. J. Phys. Oceanogr., *27,* 237–263. [the neutral density software is available at http://www.marine.csiro.au/~jackett/NeutralDensity/]

Jackett, D. R., T. J. McDougall, R. Feistel, D. G. Wright and S. M. Griffies. 2005. Updated algorithms for density, potential temperature, conservative temperature and freezing temperature of seawater. J. Phys. Oceanogr. (submitted).

Koltermann, K. P., V. Gouretski and K. Jancke. 2004. Hydrographic Atlas of the World Ocean Circulation Experiment (WOCE), Volume 3: Atlantic Ocean [www.bsh.de/aktdat/mk/AIMS].

McDougall, T. J. 1987a. Neutral surfaces. J. Phys. Oceanogr., *17,* 1950–1964.

——1987b. Thermobaricity, cabbeling, and water-mass conversion. J. Geophys. Res., *92,* 5448–5464.

——2003. Potential enthalpy: A conservative oceanic variable for evaluating heat content and heat fluxes. J. Phys. Oceanogr., *33,* 945–963.

McDougall, T. J. and D. R. Jackett. 1988. On the helical nature of neutral trajectories in the ocean. Prog. Oceanogr., *20,* 153–183.

——2005a. The thinness of the ocean in $S - \Theta - p$ space. J. Phys. Oceanogr. (submitted).

——2005b. An assessment of orthobaric density in the global ocean. J. Phys. Oceanogr. (in press).

Reid, J. L. 1994. On the total geostrophic circulation of the North Atlantic Ocean: Flow patterns, tracers, and transports. Prog. Oceanogr., *33,* 1–92.

Reid, J. L. and R. J. Lynn. 1971. On the influence of the Norwegian-Greenland and Weddell seas upon the bottom waters of the Indian and Pacific oceans. Deep-Sea Res., *18,* 1063–1088.

Sun, S., R. Bleck, C. G. H. Rooth, J. Dukowicz, E. P. Chassignet and P. Killworth. 1999. Inclusion of thermobaricity in isopycnic-coordinate ocean models. J. Phys. Oceanogr., *29,* 2719–2729.

Toole, J. M. and T. J. McDougall. 2001. Mixing and stirring in the ocean interior, *in* Ocean Circulation and Climate, G. Siedler, J. A. Church and J. Gould, eds., Pergamon, 337–355.

Received: *10 August, 2004;* revised: *27 January, 2005.*